Defects in Axonal Elongation and Neuronal Migration in Mice with Disrupted *tau* and *map1b* Genes

Yosuke Takei, Junlin Teng, Akihiro Harada, and Nobutaka Hirokawa

Department of Cell Biology and Anatomy, Graduate School of Medicine, University of Tokyo, Hongo, Bunkyo-ku, Tokyo 113-0033, Japan

Abstract. Tau and MAP1B are the main members of neuronal microtubule-associated proteins (MAPs), the functions of which have remained obscure because of a putative functional redundancy (Harada, A., K. Oguchi, S. Okabe, J. Kuno, S. Terada, T. Ohshima, R. Sato-Yoshitake, Y. Takei, T. Noda, and N. Hirokawa. 1994. *Nature.* 369:488–491; Takei, Y., S. Kondo, A. Harada, S. Inomata, T. Noda, and N. Hirokawa. 1997. *J. Cell Biol.* 137:1615–1626). To unmask the role of these proteins, we generated double-knockout mice with disrupted *tau* and *map1b* genes and compared their phenotypes with those of single-knockout mice. In the analysis of mice with a genetic background of predominantly C57Bl/6J, a hypoplastic commissural axon tract and disorganized neuronal layering were observed in the brains of the *tau*+/+*map1b*−/− mice. These phenotypes are markedly more severe in *tau*−/−*map1b*−/− double mutants, indicating that tau and MAP1B act in a synergistic fashion. Primary cultures of hippocampal neurons from *tau*−/−*map1b*−/− mice showed inhibited axonal elongation. In these cells, a generation of new axons via bundling of microtubules at the neck of the growth cones appeared to be disturbed. Cultured cerebellar neurons from *tau*−/−*map1b*−/− mice showed delayed neuronal migration concomitant with suppressed neurite elongation. These findings indicate the cooperative functions of tau and MAP1B in vivo in axonal elongation and neuronal migration as regulators of microtubule organization.

Key words: tau • MAP1B • axon • growth cone • neuronal migration

Introduction

In developing neurons projecting elongated axons over enormous distances, the cytoskeletal system in the cytoplasm, which is composed of longitudinally arranged neurofilaments and microtubules (MTs)[1], acts as a dynamic scaffold. MTs tend to form fascicles in which various kinds of crossbridge structures have been observed (Hirokawa, 1982; Hirokawa et al., 1985). Microtubule-associated proteins (MAPs), a group of filamentous proteins, have been demonstrated as components of these extensive crossbridge structures associated with MTs (Hirokawa et al., 1985, 1988; Sato-Yoshitake et al., 1989). The microtubule-associated protein 1B (MAP1B, known also as MAP1.2, MAP1X or MAP5) and tau are the main members of neuronal MAPs (Cleveland et al., 1977; Bloom et al., 1985; Noble et al., 1989). Tau is localized abundantly in axons (Hirokawa, 1994). MAP1B is evenly distributed in dendrites, cell bodies, and axons of developing nerve cells, although the localization of phosphorylated MAP1B, which is preferentially incorporated into MTs (DiTella et al., 1996), is axon dominant (Sato-Yoshitake et al., 1989; Black et al., 1994). Tau is a component of short crossbridge structures (~20 nm long) between MTs (Hirokawa et al., 1988), whereas MAP1B is a constituent of longer ones (Sato-Yoshitake et al., 1989).

Transfection analyses have revealed that tau induces elongation of processes of nonneuronal cells with the formation of MT bundles (Kanai et al., 1989; Chen et al., 1992). On the other hand, studies on the effects of tau inactivation using antisense approaches (Caceres and Kosik, 1990; Caceres et al., 1991) or chromophore-assisted laser inactivation (CALI; Liu et al., 1999) have implicated it in the establishment of neuronal polarity, axon outgrowth, and process stability. However, another study revealed that microinjection of anti-tau antibodies into cultured neurons did not result in inhibition of axonal extension (Tint et al., 1998). In regard to MAP1B, depletion of casein kinase II, which catalyzes phosphorylation of MAP1B, blocked neuritogenesis (Ulloa et al., 1993), and attenua-

Address correspondence to Nobutaka Hirokawa, Department of Cell Biology and Anatomy, Graduate School of Medicine, University of Tokyo, Hongo, Bunkyo-ku, Tokyo 113-0033, Japan. Tel.: 81-3-5841-3326. Fax: 81-3-5802-8646. E-mail: hirokawa@m.u-tokyo.ac.jp

[1]*Abbreviations used in this paper:* E, embryonic day; HE, hematoxyline-eosin; MAPs, microtubule-associated proteins; MAP1B, microtubule-associated protein 1B; MTs, microtubules; P, postnatal day.

tion of MAP1B expression by antisense oligonucleotide treatment resulted in inhibition of neurite extension in PC12 cells (Brugg et al., 1993); both suggest a role of MAP1B in neurite growth. A recent study has reported results conflicting with previous data in that axon formation in cerebellar macroneurons in culture is inhibited by treatment with a mixture of tau and MAP1B antisense oligonucleotides, but not by the single suppression by any one of the two (DiTella et al., 1996).

In parallel to these in vitro studies, efforts have also been made to elucidate the functions of MAPs in vivo by analyzing a series of knockout mice. Analysis of tau-knockout nerve cells revealed a decrease in the number of MTs in small-caliber axons, while they have extended axons indistinguishable from wild-type controls (Harada et al., 1994). Behavioral experiments of tau-deficient mice revealed muscle weakness and memory disturbance (Ikegami et al., 2000). MAP1B-deficient mice showed a delay in caliber expansion and myelination of optic nerves (Takei et al., 1997). Another group reported a more severe phenotype of MAP1B-mutant mice, namely, an early embryonic death of homozygotes at embryonic day 8 (E8) and partial postnatal lethality with brain anomalies in heterozygotes (Edelmann et al., 1996). Their data also suggest a neuronal function of MAP1B, although it is considered that the severity of the phenotypes reported by them was not a consequence of a simple loss of MAP1B function, but of a toxic effect of a truncated protein translated from the mutated gene or of other causes (Takei et al., 1997). On the other hand, a recent report showed the requirement of a MAP1B-like protein, Futsch/22C10, for neurite development in *Drosophila* (Hummel et al., 2000).

Taken collectively, these studies using knockout mice have not fully elucidated the function of tau and MAP1B in the developing mammalian nervous system, possibly because of the presence of some compensatory mechanisms in vivo. Even in vitro studies have reported conflicting results (e.g., results of studies using antisense approaches vs. microinjection of antibodies). Thus, despite considerable effort, the exact functions of tau and MAP1B in vivo have remained unclear.

Tau and MAP1B are similar not only in their effects on MT dynamics and organization in vitro (promoting tubulin assembly, binding and stabilizing MTs, and forming cross-bridge structures between MTs; Hirokawa, 1994), but also in their cellular localization in neurons. Both of them are strongly expressed in developing axons, especially in the distal part, and are colocalized with MTs in growth cones (Black et al., 1994, 1996). Thus, we generated double-knockout mice with disrupted *tau* and *map1b* genes and compared their phenotypes with those of single-knockout mice, to examine if tau and MAP1B have redundant functions in vivo, and if so, to determine what the function of tau and MAP1B as a group is. Our findings are summarized as follows: (a) dysgenesis of the axon tract with an alteration of MT constitution in vivo and suppression of axonal elongation in cultured neurons from the mutant mice; (b) MT disorganization in growth cones, which provides us new insights into the mode of action of MAPs, where and how they function with respect to the organization of MTs in axonal elongation; and (c) delayed neuronal migration resulting in perturbed neuronal layer formation, shedding light on novel aspects of the function of tau and MAP1B.

Materials and Methods

Generation of Mutant Mice

A mice line with disrupted *tau* and *map1b* genes was generated by crossing a line of tau-deficient mice (Harada et al., 1994) with one of MAP1B-deficient mice (Takei et al., 1997). Analyzed mice had a C57Bl/6J (>93%) ×129/Sv (<7%) background. Although spontaneous agenesis of the corpus callosum has been reported in some inbred strains of mice, including the 129/ReJ and 129/J lines, the C57Bl/6J×129/Sv hybrid line does not exhibit a significant incidence of agenesis of the corpus callosum (Wahlsten, 1989). The genotype of the mice was determined by PCR of genomic DNA as previously described (Harada et al., 1994; Takei et al., 1997).

Light Microscopy

Age-matched mice were anesthetized with ether and transcardially perfused with Bouin's solution. Brain tissues were dissected out, dehydrated through a graded alcohol series, cleared with xylene, and embedded in Paraplast (Oxford Labware). The tissues were serially sectioned (7 μm thick) and stained by the Bodian method, a silver stain procedure for visualizing nerve fibers (Bodian, 1936), or the hematoxyline-eosin (HE) method. Samples were microphotographed using an Optiphoto-2 microscope (Nikon).

Electron Microscopy

Mice were anesthetized and transcardially perfused with 2% paraformaldehyde and 2.5% glutaraldehyde in 0.1 M cacodylate buffer. Brain tissues were dissected out, fixed overnight, processed by the conventional method, and viewed under a JEOL 1200EX electron microscope at 100 kV. Matching areas of each tissue were examined and photographed, and then the areas of axons and the numbers of MTs were directly measured and counted, respectively, from prints. The number of MTs was then converted to the density of MTs by dividing the counts by each axonal area.

Culture of Hippocampal Neurons

The hippocampi of E16.5 fetuses were dissected and cultured as described previously (Harada et al., 1994). The cells were plated at a density of 50,000 cells per 35-mm dish. The neurons were directly microphotographed by diaphoto phase-contrast microscopy (Nikon) or observed after immunostaining. The length and the number of neurites were measured from immunofluorescence micrographs of the cells stained with an anti-tubulin antibody, and for the growth cone area, with phalloidin.

In Vitro Migration Assay

The cerebelli of postnatal day 0.5 (P0.5) pups were dissected and cerebellar aggregates were generated as described previously (Kobayashi et al., 1995; Bix and Clark, 1998). Dissociated cerebellar granule cells form aggregate spheres that adhere to the laminin substrate during the first hour of plating. Neuronal processes extend from the aggregates. After several hours, small bipolar granule cells migrate unidirectionally away from the cell clusters along these neurites, followed by translocation of cell bodies outside the aggregate margin. The neurons were directly photographed by diaphoto phase-contrast microscopy (Nikon) or observed after immunostaining.

Immunocytochemistry

Immunocytochemistry was performed using a standard method as described previously (Tanaka et al., 1992). Samples were observed using a laser scanning confocal microscope (model MRC-1000; Bio-Rad) or an axiovert microscope (Carl Zeiss). The following monoclonal antibodies were used as the primary antibodies: 1B9 (Sato-Yoshitake et al., 1989) for phosphorylated MAP1B, tau-1 (Boehringer Mannheim) for tau. Cy3-conjugated anti-mouse IgG (Amersham Life Science) were used as the secondary antibody. FITC-conjugated phalloidin (Sigma-Aldrich) was used for staining F-actin.

Results

Postnatal Letality in *tau +/+map1b −/−* and *tau −/−map1b −/−* Mice

Tau +/−map1b +/− mice grew with no apparent abnormalities. Their brain sections at 6 mo of age were histologically indistinguishable from those of *tau +/+map1b +/+* mice (data not shown). To generate *tau −/−map1b −/−* mice, we crossed male and female *tau +/−map1b +/−* mice and determined the genotypes of their pups. We found a predicted Mendelian distribution of genotypes when we examined pups at E16.5 and P0.5 (Table I; $P > 0.9$, as determined by chi-square for independence test). However, when we performed PCR of the tail genomes of 4-wk-old mice, the results deviated from the Mendelian distribution (Table I). Interestingly, a large percentage of the *tau +/+ map1b −/−* mice (∼40% of the total) died before they reached 4 wk of age (Table I). This differed from results reported previously, where *tau +/+map1b −/−* mice did not exhibit any significant postnatal lethality (Takei et al., 1997). This discrepancy is probably attributable to the change in the genetic background of mice used. In our previous work, we used mice with a genetic background of C57Bl/6J×129/Sv hybrid (50%/50%), whereas in this research we used mice whose genetic background was predominantly C57Bl/6J (>93%), generated by repeated backcrosses with C57Bl/6J mice. All of the following data, including the reexamination of single-knockout mice, were collected using mice with this genetic background. A considerably high incidence of postnatal death was also seen in *tau +/−map1b −/−* (∼40% of total) and *tau −/− map1b −/−* (∼80% of total) mice (Table I). Malnutrition and dehydration may be the cause of postnatal death, since *tau +/+map1b −/−*, *tau +/−map1b −/−*, and *tau −/− map1b −/−* mice often showed a lack of milk in their stomach (Fig. 1). Adult *tau +/+map1b −/−* and *tau −/− map1b −/−* mice displayed a slight drooping of their upper eyelids (blepharoptosis-like symptom), which was previously reported in *tau +/+map1b −/−* mice (Takei et al., 1997).

Table I. Genotype Distribution of Offspring after Mutual tau +/−map1b +/− Mating

Age	Number of progeny			Mendelian distribution
	E16.5	P0.5	4 wk*	
tau +/+map1b +/+	11 (8.7%)	24 (5.8%)	54 (9.7%)	6.25%
tau +/−map1b +/+	17 (13.4%)	47 (11.3%)	80 (14.4%)	12.5%
tau −/−map1b +/+	9 (7.1%)	29 (7.0%)	40 (7.2%)	6.25%
tau +/+map1b +/−	17 (13.4%)	54 (12.9%)	86 (15.5%)	12.5%
tau +/−map1b +/−	34 (26.8%)	102 (24.5%)	162 (29.2%)	25%
tau −/−map1b +/−	11 (8.7%)	66 (15.8%)	64 (11.6%)	12.5%
tau +/+map1b −/−	8 (6.3%)	24 (5.8%)	20 (3.6%)	6.25%
tau +/−map1b −/−	10 (7.9%)	44 (10.6%)	42 (7.6%)	12.5%
tau −/−map1b −/−	10 (7.9%)	27 (6.5%)	6 (1.1%)	6.25%
Total	127	417	554	

Numbers of pups of each genotype are shown.
*Differs from Mendelian distribution at $P < 0.001$ using Chi-square for independence test.

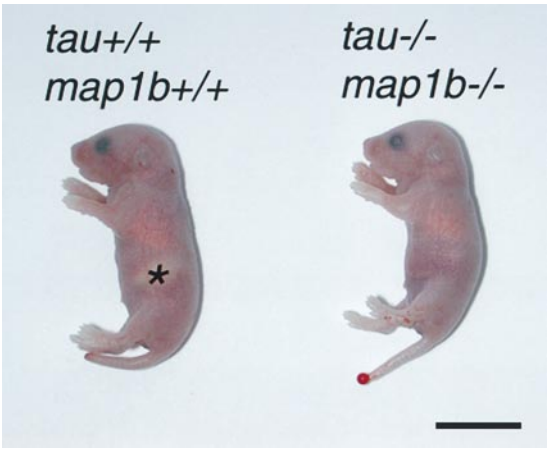

Figure 1. Gross appearance of *tau +/+map1b +/+* and *tau −/− map1b −/−* mice (P0.5). Note the lack of milk in the stomach of the *tau −/−map1b −/−* animal. The area indicating stomach filled with milk in the *tau +/+map1b +/+* mouse is marked with an asterisk. Bar, 10 mm.

Brain Anomalies in MAP-mutant Mice

The whole-brain weights (cerebrum + cerebellum) of *tau +/+map1b +/+*, *tau −/−map1b +/+*, *tau +/+map1b −/−*, and *tau −/−map1b −/−* mice were measured at P0.5 and 4 weeks of age. There is no significant difference in the whole-brain weights between *tau +/+map1b +/+* and *tau −/−map1b +/+* mice (Table II; $P > 0.7$ at P0.5 and $P > 0.4$ at 4 weeks of age, as determined by Scheffe's post-hoc test). The whole-brain weight of *tau +/+map1b −/−* mice was significantly smaller than that of *tau +/+map1b +/+* mice (Table II; $P < 0.05$ at P0.5 and $P < 0.001$ at 4 wk of age, as determined by Scheffe's post-hoc test). Whereas there was no significant difference in the whole-brain weights between *tau +/+map1b −/−* and *tau −/−map1b −/−* mice at P0.5, a significant difference in the values between the mice was observed at 4 wk of age (Table II), indicating that the difference in whole-brain weight becomes apparent during postnatal development.

Histological analysis of the brain sections revealed abnormalities of the axon tract of the *tau +/+map1b −/−* and *tau −/−map1b −/−* mice (Fig. 2). Severe dysgenesis of the forebrain commissural fiber bundles, corpus callosum, anterior commissure, and hippocampal commissure, which connect the left and right cerebral hemispheres, was observed in the brains of the *tau −/−map1b −/−* mice (Fig. 2,

Table II. Brain Weight of Mice

Age	P0.5	4 wk
	g	
tau +/+map1b +/+	0.11 ± 0.01 (5)‡	0.46 ± 0.01 (9)‡
tau −/−map1b +/+	0.10 ± 0.003 (11)‡	0.44 ± 0.01 (4)‡
tau +/+map1b −/−	0.08 ± 0.01 (5)	0.38 ± 0.01 (11)*
tau −/−map1b −/−	0.08 ± 0.002 (14)	0.34 ± 0.01 (4)

Whole brain weight (cerebrum + cerebellum). The means ± SEM (number of mice examined) are shown.
*Differs from *tau −/−map1b −/−* at $P < 0.05$.
‡Differs from *tau −/−map1b −/−* at $P < 0.001$ using Scheffe's post-hoc analysis.

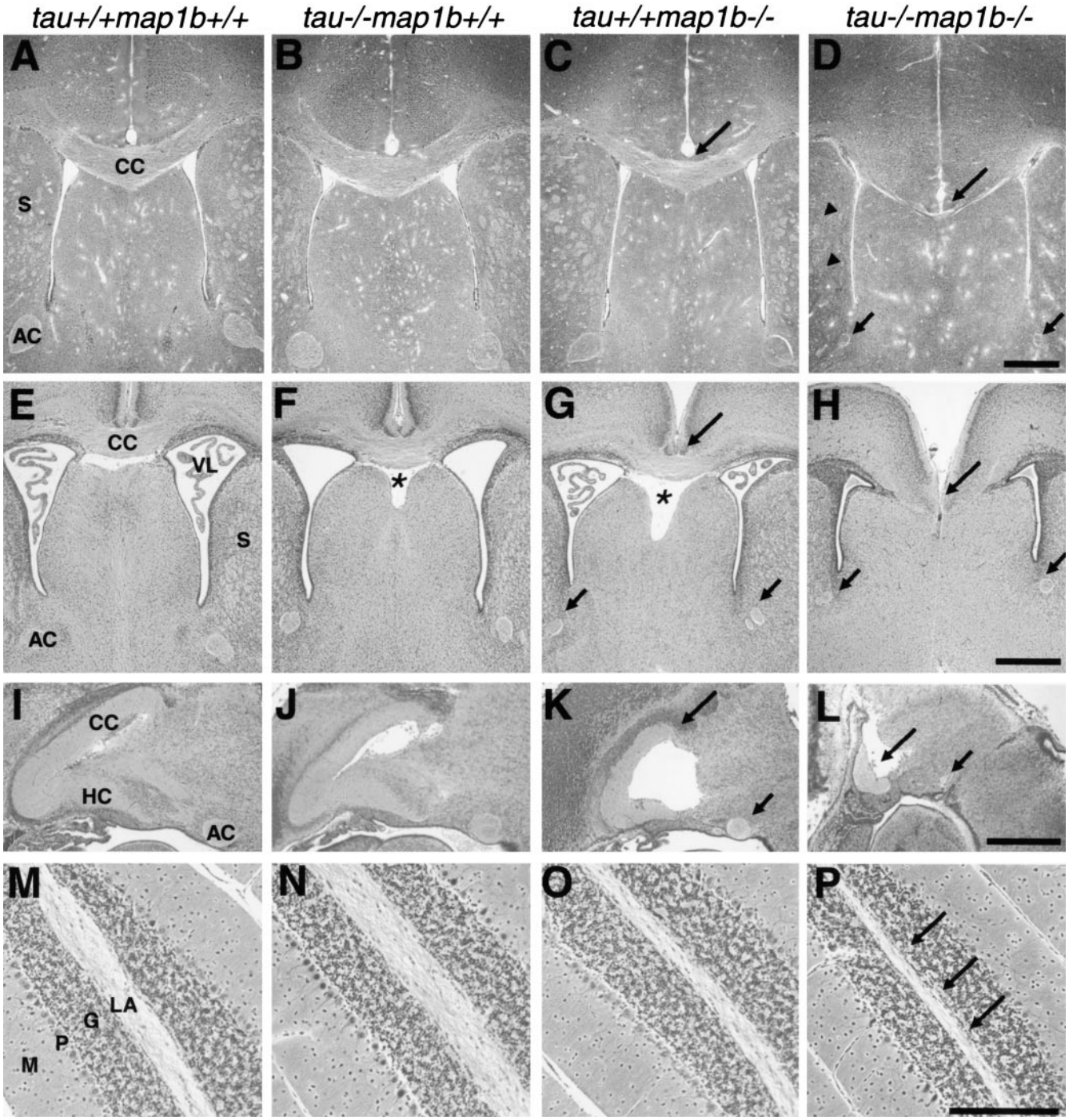

Figure 2. Defects of axon tract formation in mutant mice. Sections of paraffin-embedded brains of *tau+/+map1b++*, *tau−/−map1b+/+*, *tau+/+map1b−/−*, and *tau−/−map1b−/−* mice killed at 4 weeks (A–D, M–P) or 0.5 day (E–L) of age. Bodian silver staining (A–H, M–P) or HE staining (I–L). (A–L) Micrographs showing representative areas in frontal (A–H) or mid-sagittal (I–L) sections of the cerebrum. Note the decreased size of the corpus callosum (long arrows) and the anterior commissure (short arrows) in the brains of *tau+/+map1b−/−* mice (C, G, and K) and their severe dysgenesis in the brains of *tau−/−map1b−/−* mice (D, H, and L). Arrowheads in D point the hypoplastic tracts in the striatum. Asterisks indicate the enlarged cavum septi pellucidi (F and G). (M–P) Sagittal sections of the cerebellum. Note that the size of the linea alba is significantly decreased in the brains of *tau−/−map1b−/−* mice (arrows in P). AC, anterior commissure; CC, corpus callosum; G, granular cell layer; HC, hippocampal commissure; LA, linea alba; M, molecular layer; P, Purkinje cell layer; S, striatum; VL, ventriculus lateralis. Bars: (D, H, and L) 0.5 mm; (P) 100 μm.

D, H, and L, long and short arrows). Brains of *tau+/+map1b−/−* mice also exhibited a reduction in the size of these structures (Fig. 2 C, G, and K, long and short arrows). The severity of the commissure defects in *tau−/−map1b−/−* mice was significantly severer than those in *tau+/+map1b−/−* mice, which was clearly shown by a quantitative comparison of the cross-sectional area of the commissural fiber tract at the midsagittal plane (Table

Table III. Forebrain Commissure Size

	Corpus callosum + hippocampal commissure	Anterior commissure	*n*
	mm^2		
tau +/+map1b +/+	1.40 ± 0.05*	0.14 ± 0.004*	12
tau −/−map1b +/+	1.26 ± 0.09*	0.14 ± 0.01*	16
tau +/+map1b −/−	0.81 ± 0.04*	0.08 ± 0.01‡	19
tau −/−map1b −/−	0.30 ± 0.07	0.04 ± 0.01	10

Cross-sectional areas of major forebrain fibre tracts at the midsagittal plane were measured at the age of P0.5. Because the boundary between the corpus callosum and the hippocampal commissure of dyscallosal animals is difficult to determine, the combination of the two regions were compared. The means ± SEM are shown. *n*, Number of mice examined.
*Differs from *tau −/−map1b −/−* at $P < 0.001$ using Scheffe's post-hoc analysis.
‡Differs from *tau −/−map1b −/−* at $P < 0.01$.

III). The size of commissural fiber tracts of *tau −/− map1b +/+* mice did not differ from that of *tau +/+ map1b +/+* mice (Fig. 2, B, F, and J, and Table III; corpus callosum+hippocampal commissure, $P > 0.8$; anterior commissure, $P > 0.9$, as determined by Scheffe's post-hoc test).

Noncommissural axon tracts such as tracts in the striatum (Fig. 2 D, arrowheads), cerebellar white matter (linea alba; Fig. 2 P, arrows), and tracts of the spinal cord (data not shown), were also hypoplastic in *tau −/−map1b −/−* mice. In addition, the cavum septi pellucidi was enlarged in the *tau −/−map1b +/+* and *tau +/+map1b −/−* mice at P0.5 (Fig. 2, F and G, asterisks).

Defects in the neuronal layer structures were another striking abnormality in the brains of the *tau +/+map1b −/−* and *tau −/−map1b −/−* mice (Fig. 3). The hippocampal pyramidal cell layer in the brains of *tau +/+map1b −/−* mice showed a split in the CA1 region (Fig. 3, C and G, arrows), which is also a characteristic feature of *reeler* and mDab1-deficient mice (Trommsdorff et al., 1999). Tissue sections from the *tau −/−map1b −/−* mice exhibited more drastic layering defects than those of *tau +/+map1b −/−* mice, distorted shape of hippocampus (Fig. 3, D and L),

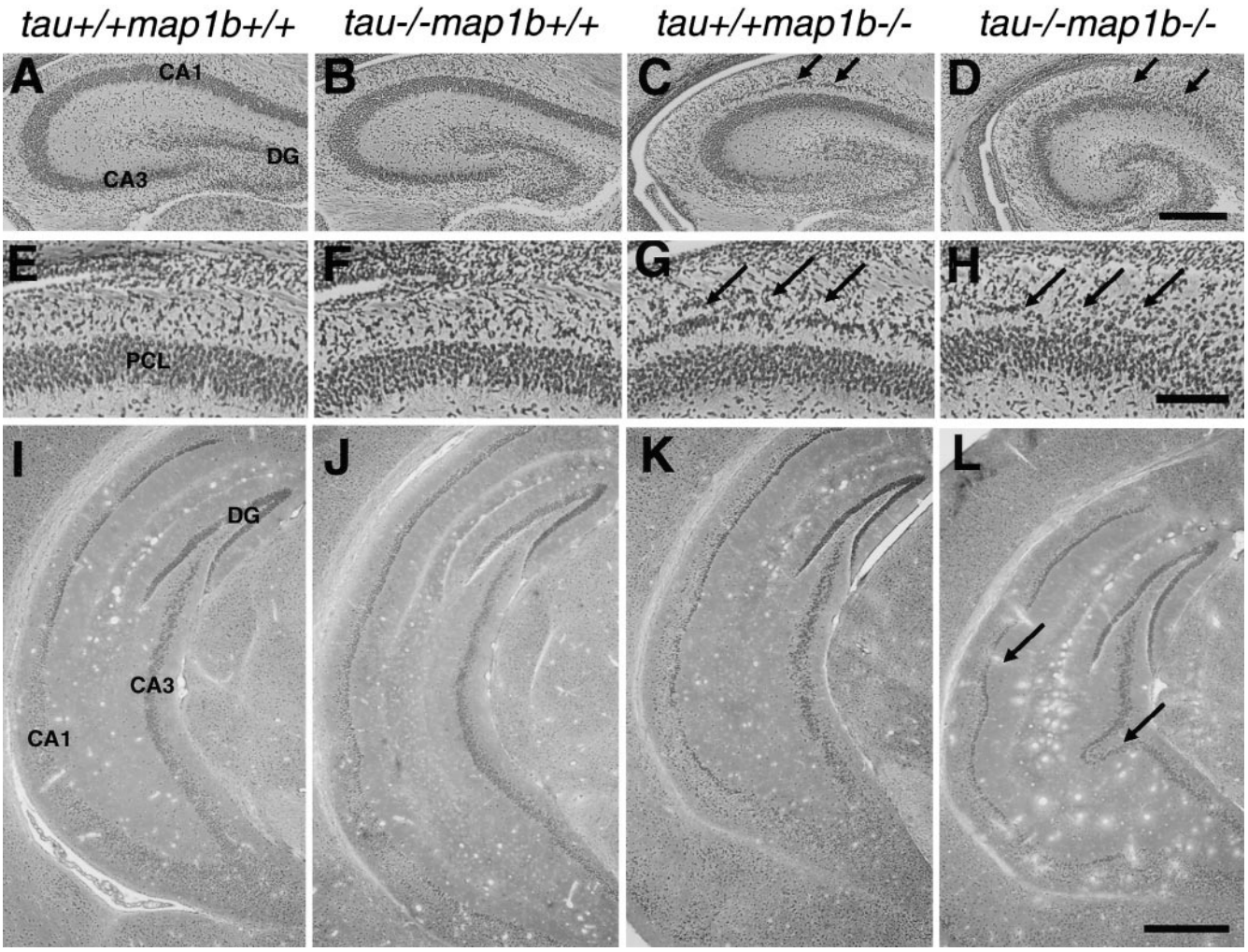

Figure 3. Defects of neuronal layer formation in mutant mice. Sections of paraffin-embedded brains of *tau +/+map1b ++*, *tau −/− map1b +/+*, *tau +/+map1b −/−*, and *tau −/−map1b −/−* mice killed at 0.5 d (A–H) and 4 wk (I–L) of age, stained by Bodian method. Note that neuronal cell bodies in the pyramidal cell layer are loosely associated with each other (D and H, arrows), and the pyramidal cell layer is undulated (L, arrows) in the brains of *tau −/−map1b −/−* mice. Arrows in C and G indicate the split in the pyramidal cell layer in the brains of *tau +/+map1b −/−* mice. CA, cornu ammonis; DG, dentate gyrus; and PCL, pyramidal cell layer. Bars: (D) 0.25 mm; (H) 0.1 mm; (L) 0.5 mm.

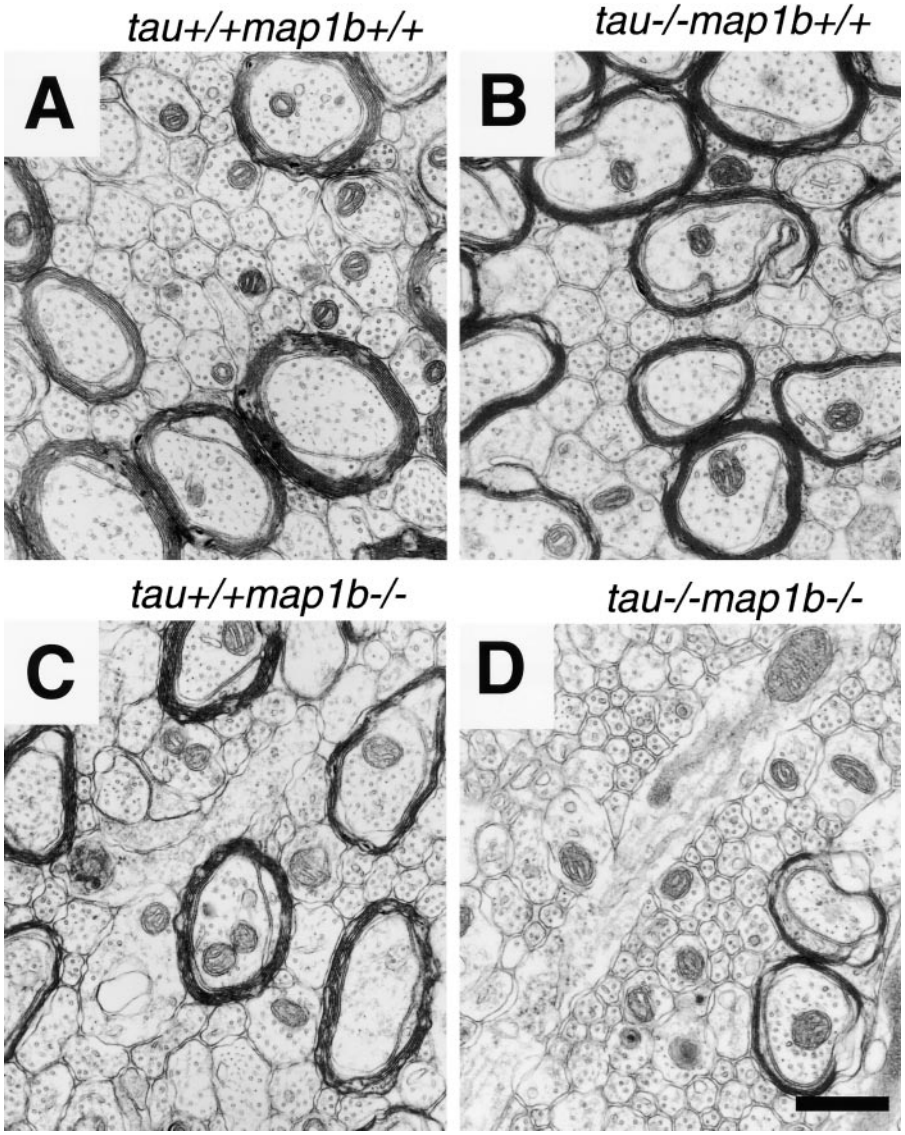

Figure 4. Drastic reduction in area of axons and MT number per axon in neurons of *tau −/− map1b −/−* mice. (A–D) Electron micrographs showing representative areas in cross sections of the anterior commissure of *tau +/+ map1b + +*, *tau −/− map1b +/+*, *tau +/+ map1b −/−*, and *tau −/− map1b −/−* mice at postnatal week 4. Bar, 0.5 μm.

loose association of pyramidal neurons throughout the pyramidal cell layer (Fig. 3, D and H, arrows), and undulated pyramidal cell layer (Fig. 3 L, arrows).

Suppressed Axonal Development with Decreased Number of MTs

We next analyzed the anterior commissures by electron microscopy to investigate in detail the axonal structures in the mutant brains (Fig. 4 and Table IV). In two independent experiments (#1 and #2), the cross-sectional area of axons and the MT number per axon of *tau −/− map1b −/−* mice were greatly reduced (Fig. 4 D and Table IV). The differences in these parameters between *tau −/− map1b −/−* mice and mice of other genotypes were statistically significant (Table IV). The density of MTs (MT number per axonal area) was, however, not significantly changed (*tau +/+ map1b +/+*, 101 ± 3 (223), *tau −/− map1b −/−*,

Table IV. Quantitative Comparison of MT Number and Cross-sectional Area of Axons

	#1			#2		
Experiments	MT number	Area of axons	*n*	MT number	Area of axons	*n*
tau +/+ map1b +/+	7.8 ± 0.4*	0.091 ± 0.006*	223	6.7 ± 0.2 *	0.068 ± 0.003*	322
tau −/− map1b +/+	5.7 ± 0.2*	0.089 ± 0.005*	227	6.8 ± 0.3 *	0.082 ± 0.005*	239
tau +/+ map1b −/−	5.6 ± 0.2*	0.060 ± 0.003*	425	5.2 ± 0.2 *	0.067 ± 0.003*	480
tau −/− map1b −/−	2.4 ± 0.1	0.035 ± 0.002	710	2.6 ± 0.1	0.036 ± 0.002	663

MT number and area of axons (μm^2) per axon were measured directly on electron-microscopic micrographs of anterior commissure sections in two independent experiments (#1 and #2). The mice were killed at postnatal week 4. The means ± SEM are shown. *n*, Number of axons examined.
*Differs from *tau −/− map1b −/−* at $P < 0.001$ using Scheffe's post-hoc analysis.

97 ± 2 (710); mean ± SEM (n)/μm^2; $P = 0.29$ by Student's t test). These data show that axonal development was inhibited in association with altered MT constitutions in *tau −/−map1b −/−* mice.

Inhibited Neurite Outgrowth in Cultured Neurons

To compare the neurite development of control and mutant mice, cultured hippocampal neurons were analyzed. This culture system enabled us to investigate the polar development of neurons maintained separately from glias (Dotti et al., 1988). Within 1 d after plating, majority of these neurons had several extended minor processes. Within another few days, they had a single growing axon, which continued to elongate (Fig. 5). We examined the expression of tau and MAP1B in these neurons from *tau +/+ map1b +/+* (Fig. 6, A–D) and *tau −/−map1b −/−* (Fig. 6, E–H) mice by double-staining with FITC-conjugated phalloidin (Fig. 6, A, C, E, and G), and also antibodies against tau (Fig. 6, B and F) or phosphorylated MAP1B (Fig. 6, D and H). In neurons from *tau +/+map1b +/+* mice, both tau and phosphorylated MAP1B were localized in an axon-dominant fashion, as reported previously (Black et al., 1994, 1996; Fig. 6, B and D), whereas neurons from *tau −/−map1b −/−* mice exhibited no immunoreactivity to the antibodies used (Fig. 6, F and H). These data imply the presence of tau and MAP1B in the neurons of *tau +/+ map1b +/+* mice and their absence in those of *tau −/− map1b −/−* mice.

Next, to assess the effect of *tau* and *map1b* mutation on neuronal differentiation, we measured the fraction of neurons at stage 3 (stage of axonal elongation; Dotti et al., 1988). Although a significant difference in the percentage of neurons at stage 3 was observed between cultures from *tau +/+map1b +/+* and *tau −/−map1b −/−* mice, a proportion of neurons from *tau −/−map1b −/−* mice are polarized (Table V), with a single axon-like process distinguishable from the minor processes (Fig. 5, arrows). *Tau −/−map1b +/+* and *tau +/+map1b −/−* neurons did not significantly differ from *tau +/+map1b +/+* neurons in the percentage of neurons at stage 3 (Table V; $P > 0.9$ and $P > 0.2$, respectively, determined by Scheffe's post-hoc test). We performed a morphometric analysis of the neurons at stage 3. The number of processes per cell was not altered between cells from the different genotypes (Table VI; $P > 0.15$, as determined by one-way ANOVA). The axonal length of neurons from *tau −/−map1b −/−* mice was the shortest among those from the four genotypes (Fig. 5 and Table VI). A decrease in average axonal length of cells from *tau +/+map1b −/−* mice was shown, although this was not statistically significant (Fig. 5 and Table VI; $P > 0.05$, as determined by Scheffe's post-hoc test). The difference between neurons from *tau +/+map1b −/−* and *tau −/−map1b −/−* mice was statistically significant (Table VI). As reported previously (Harada et al., 1994), there was no significant difference in the axonal length between cultures from *tau +/+map1b +/+* and *tau −/−map1b +/+* mice (Fig. 5 and Table VI; $P > 0.9$, as determined by Scheffe's post-hoc test). The extension of minor processes was also affected in neurons from *tau +/+map1b −/−* and *tau −/−map1b −/−* mice (Fig. 5 and Table VI). *Tau +/+ map1b −/−* and *tau −/−map1b −/−* neurons differed significantly from *tau +/+map1b +/+* neurons in the length of minor process (Table VI; $P < 0.01$ and $P < 0.001$, respectively, determined by Scheffe's post-hoc test). There was no significant difference between neurons from *tau −/− map1b +/+* and *tau +/+map1b +/+* mice (Table VI; $P >$

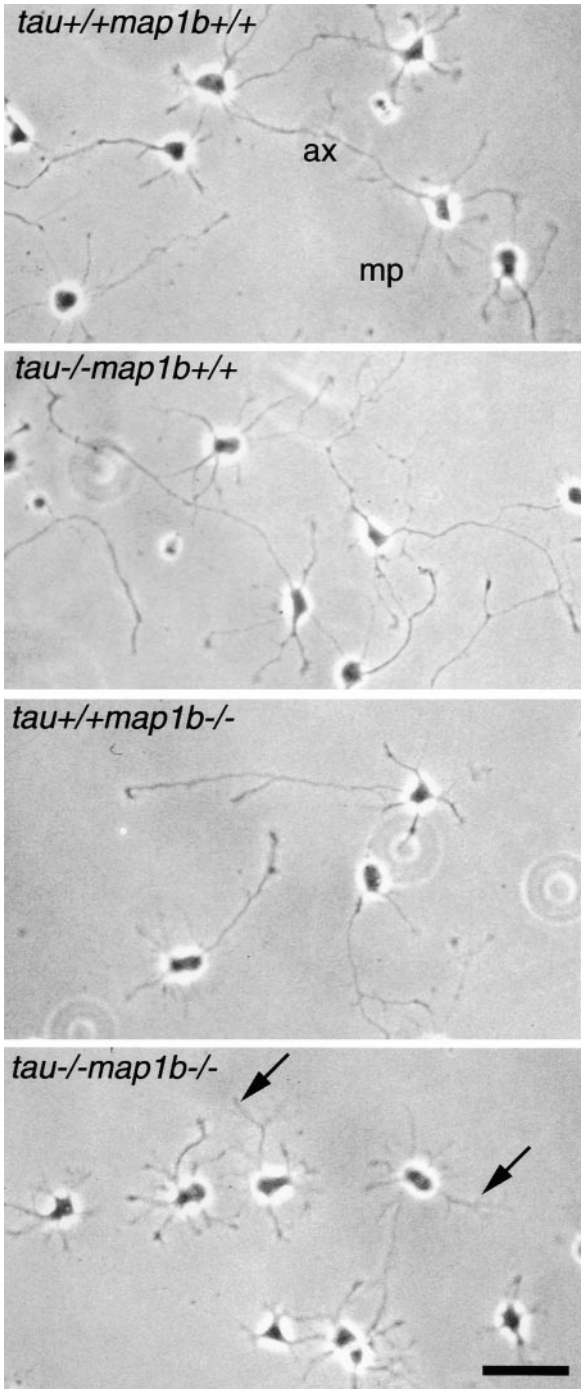

Figure 5. Phenotypes of hippocampal neurons in culture. Hippocampal neurons obtained from *tau +/+map1b ++*, *tau −/− map1b +/+*, *tau +/+map1b −/−*, and *tau −/−map1b −/−* mice were cultured for 3 d and observed by phase-contrast microscopy. Axonal outgrowth of cells from *tau −/−map1b −/−* mice was significantly inhibited (arrows). ax, axon; and mp, minor process. Bar, 50 μm.

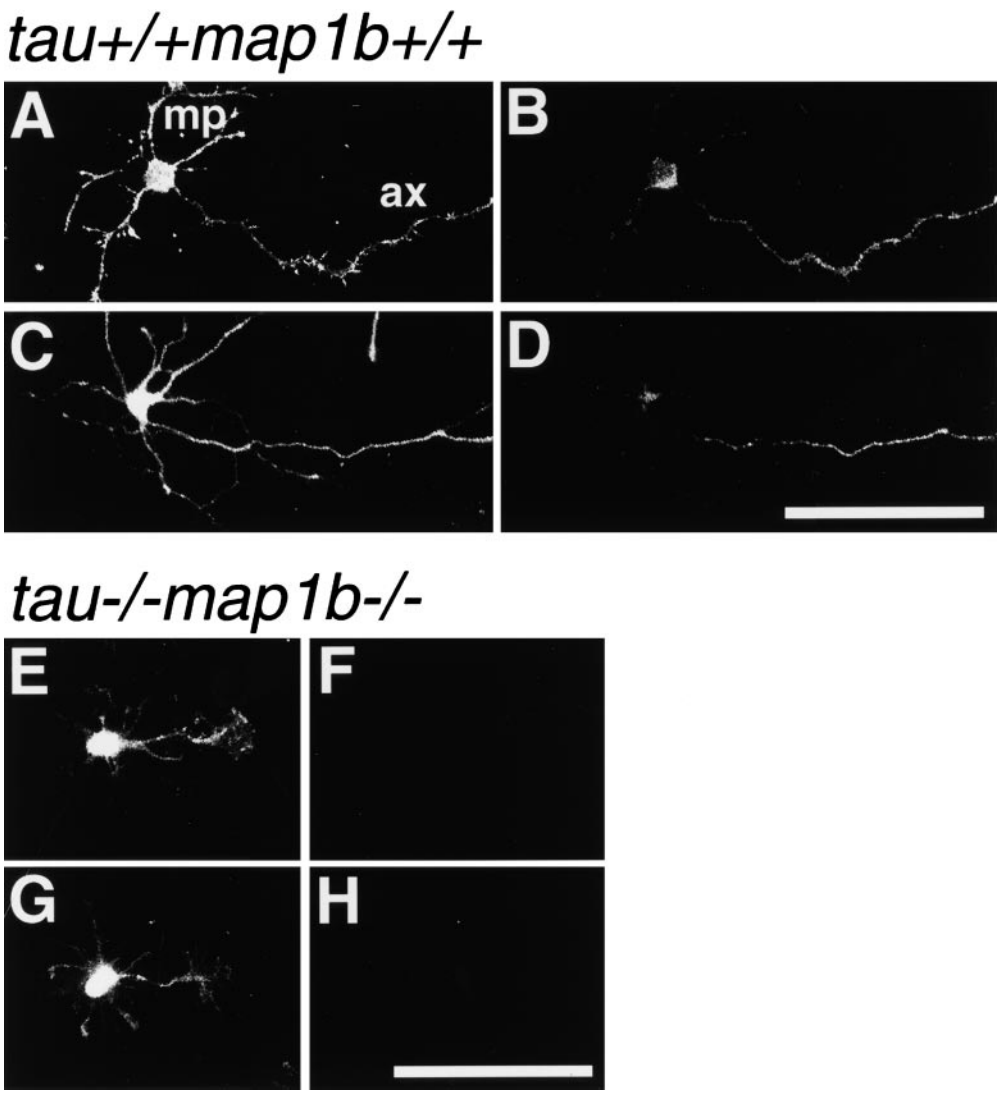

Figure 6. Expression and cellular localization of tau and MAP1B in hippocampal cells. Neurons from *tau+/+ map1b+/+* (A–D) or *tau−/− map1b−/−* mice (E–H), cultured for 3 d, were double-labeled with phalloidin (A, C, E, and G) and monoclonal antibodies recognizing the tau-1 epitope (B and F) or phosphorylated MAP1B (D and H). Both immunoreactivities are axon-dominant in the cells of *tau+/+map1b +/+* mice (B and D), whereas they are negative in the cells from *tau−/− map1b−/−* mice (F and H). ax, axon; and mp, minor process. Bars, 50 μm.

0.9, determined by Scheffe's post-hoc test). *Tau+/+ map1b−/−* and *tau−/−map1b−/−* neurons did not significantly differ in the length of minor processes ($P > 0.7$, determined by Scheffe's post-hoc test). Thus, we concluded that tau and MAP1B act cooperatively in axonal elongation, but not in minor process elongation, where the null mutation of *tau* gene has little effect.

Table V. Effect of tau and map1b Mutation on Neuronal Differentiation in Cultured Hippocampal Neurons

	Percentage of neurons at stage 3	*n*
tau+/+map1b+/+	88.7 ± 2.4*	6
tau−/−map1b+/+	86.3 ± 2.7‡	4
tau+/+map1b−/−	80.4 ± 2.4	4
tau−/−map1b−/−	73.4 ± 2.1	5

Percentage of cells at stage 3 (stage of axonal elongation). Cells stained with a monoclonal antibody against tubulin were examined. *n*, number of animals examined. A total of 100–160 cells per animal were analyzed. The means ± SEM are shown.
*Differs from *tau−/−map1b−/−* at $P < 0.01$. Scheffe's post-hoc analysis.
‡Differs from *tau−/−map1b−/−* at $P < 0.05$.

MT Disorganization and Altered Growth Cone Morphology

To investigate the cytoskeletal organization of cultured cells, we double-stained neurons with an anti-tubulin antibody and phalloidin, because actin microfilaments and

Table VI. Effect of tau and map1b Mutation on Neurite Development in Cultured Hippocampal Neurons

	Neurite length			
	Axon	Minor process	No. of neurites	*n*
	μm			
tau+/+map1b+/+	172.5 ± 10.8*	37.8 ± 2.7*	6.2 ± 0.1	6
tau−/−map1b+/+	167.5 ± 9.9*	36.9 ± 2.3‡	6.0 ± 0.1	4
tau+/+map1b−/−	135.8 ± 4.4*	25.2 ± 1.5	5.3 ± 0.4	4
tau−/−map1b−/−	62.6 ± 8.0	22.0 ± 0.9	5.7 ± 0.4	5

Values in each hippocampal neuron were measured directly on immunofluorescence micrographs of the cells stained using a monoclonal antibody against tubulin. *n*, Number of animals examined. 30 cells in stage 3 per animal were analyzed. The means ± SEM are shown.
*Differs from *tau−/−map1b−/−* at $P < 0.001$. Scheffe's post-hoc analysis.
‡Differs from *tau−/−map1b−/−* at $P < 0.01$.

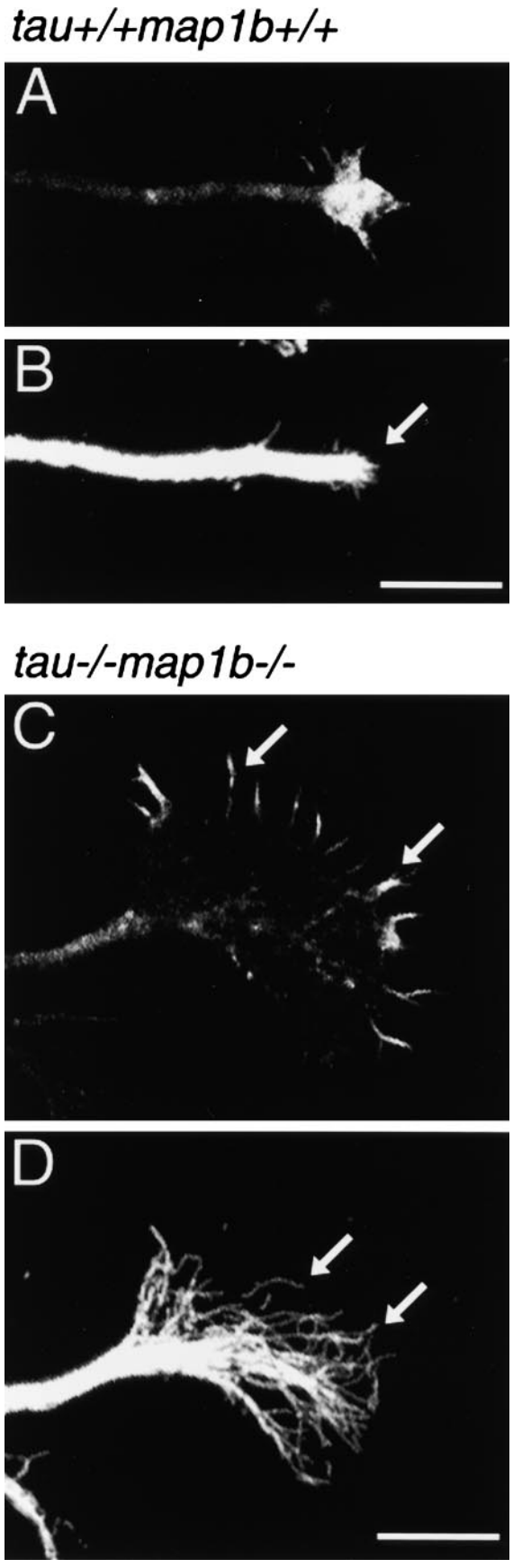

Figure 7. Cytoskeletal organization in growth cones. Growth cones of hippocampal neurons from *tau+/+map1b+/+* (A and B) or *tau−/−map1b−/−* (C and D) mice cultured for 3 d were double-labeled with phalloidin (A and C) and a monoclonal antibody against tubulin (B and D). Note that the growth cone of hippocampal neurons from *tau−/−map1b−/−* mice is extensive (C), throughout which MTs are flared out (D, arrows), instead of being bundled as seen in the neurons from *tau+/+map1b+/+* mice (B, arrow). Bars, 10 μm.

Table VII. Quantitative Comparison of Growth Cone Areas

	Area of growth cones	*n*
	μm^2	
tau+/+map1b+/+	73.2 ± 10.6‡	4
tau−/−map1b+/+	67.8 ± 4.5‡	4
tau+/+map1b−/−	103.5 ± 13.4*	4
tau−/−map1b−/−	228.0 ± 19.3	4

Areas of the largest axonal growth cones in each neurons were measured directly from immunofluorescence micrographs of cells stained with FITC-phalloidin and analyzed. *n*, Number of animals examined. Thirty cells per animal were analyzed. The means ± SEM are shown.
*Differs from *tau−/−map1b−/−* at $P < 0.05$.
‡Differs from *tau−/−map1b−/−* at $P < 0.01$. Scheffe's post-hoc analysis.

MTs are the major determinants of neuronal shape (Tanaka and Sabry, 1995). Cultured neurons from *tau−/−map1b−/−* mice exhibited a striking feature in their growth-cone morphology as well. The growth cone situated at the tip of axon-like processes in neurons of *tau−/−map1b−/−* mice cultured for 3 d often exhibited an extended form (Fig. 7, C and D). The difference in the areas of the growth cones between *tau−/−map1b−/−* mice and mice of other genotypes was statistically significant (Table VII). *Tau−/−map1b+/+* and *tau+/+map1b−/−* neurons did not significantly differ from *tau+/+map1b+/+* neurons in the areas of the growth cones ($P > 0.9$ and $P > 0.5$, respectively, determined by Scheffe's post-hoc test).

In the neurons from *tau+/+map1b+/+* mice, the MTs in the growth cones at the tip of developing axons tended to bundle together rather tightly around the central region in the growth cones (Fig. 7 B, arrow). The neurons from *tau−/−map1b−/−* mice, however, had a quite different MT organization, where the MTs were splayed into single MTs with a slight tendency toward bundling, especially in the peripheral region of the growth cones (Fig. 7 D, arrows). F-actin in the growth cones of *tau−/−map1b−/−* mice was localized mainly in the filopodia, and not in the central MT-rich domain (Fig. 7 C, arrows), which differed strikingly from the case in the neurons from *tau+/+map1b+/+* mice (Fig. 7 A). From these data, we concluded that a cytoskeletal disorganization, mainly of the MTs, and also of actin filaments, was related to the abnormal shape of the growth cones in the *tau−/−map1b−/−* mice.

Delay in Migration of tau−/−map1b−/− Neurons

Histological analyses of *tau−/−map1b−/−* brains suggested the presence of a migration defect in *tau−/−map1b−/−* neurons. To elucidate this by comparing migration of *tau−/−map1b−/−* neurons with that of *tau+/+map1b+/+* neurons, we examined the unidirectional in vitro migration of granule cells from cerebellar cell reaggregates on a laminin substrate (Bix and Clark, 1998;

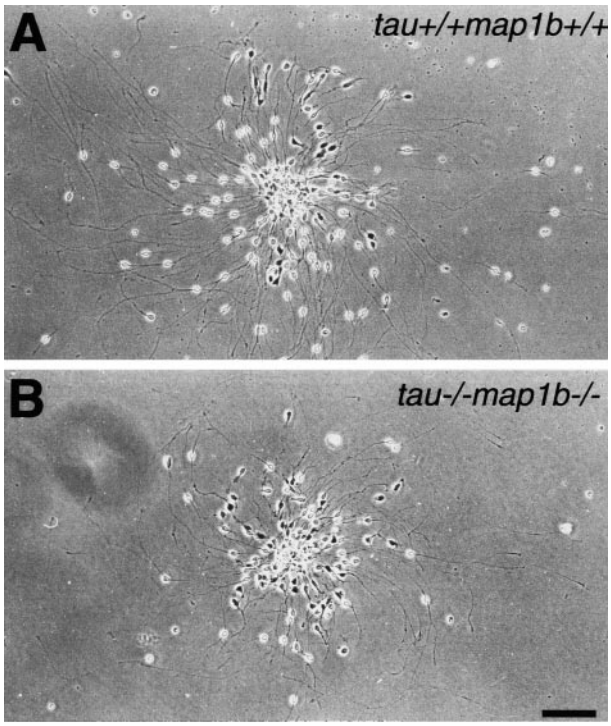

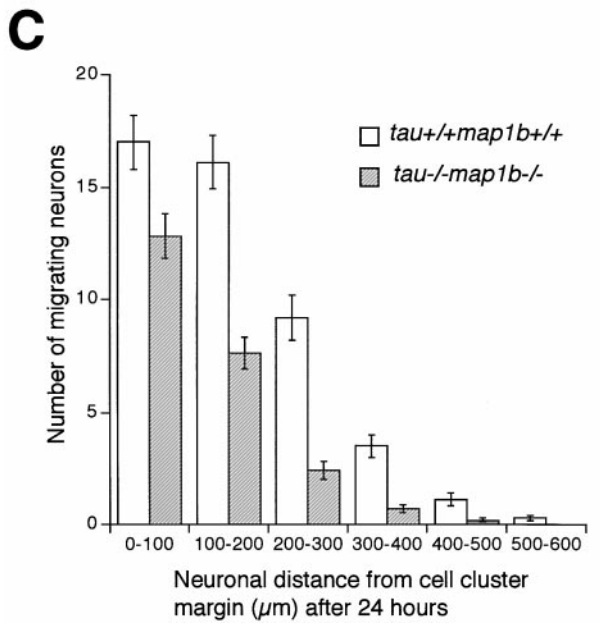

Figure 8. In vitro analysis of neuronal migration. Migration of *tatau +/+map1b +/+* (A) and *tau −/−map1b −/−* (B) cerebellar granule cells from reaggregate cell clusters after 24 h of culture. (C) Mean ± SEM of the number of migrating cerebellar granule cells and their distance of migration from the reaggregate cell cluster in *tau +/+map1b +/+* and *tau −/−map1b −/−* mice after 24 h. Three animals of each genotype were used, and 35 *tau +/+ map1b +/+* and 33 *tau −/−map1b −/−* clusters were examined. Bar, 100 μm.

Kobayashi et al., 1995). Cerebellar granule cells can be easily identified by their bipolar, spindle-shaped morphology with neurites. These neurites were positive for tau and MAP1B immunoreactivities as revealed by immunofluorescence (data not shown). There was a striking difference between the migration of *tau +/+map1b +/+* (Fig. 8 A) and *tau −/−map1b −/−* (Fig. 8 B) neurons from reaggregate clusters. We measured the distance that each neuron migrated after 24 h for each genotype, and confirmed quantitatively that mutant cells migrated at shorter distances than wild-type cells (Fig. 8 C). There were significant differences in migration distances from the cluster margin after 24 h between neurons derived from *tau +/+ map1b +/+* and *tau −/−map1b −/−* mice ($P < 0.001$ by the Mann-Whitney rank sum test). No significant difference was observed in the size of cell clusters between genotypes (*tau +/+map1b +/+*; 38.4 ± 1.4 (35), *tau −/−map1b −/−*; 35.9 ± 1.6 (33), mean ± SEM (number of aggregates examined) μm, $P > 0.2$, Student's *t* test). As neurites serve as the migration substrate for neurons, neurite lengths were compared between genotypes and a significant difference in the mean length of neurites were observed (Table VIII). We compared the migration index, defined as the ratio of the number of neurons that migrated over one-third of the neurite length to the total number of migrating neurons (Kobayashi et al., 1995), to evaluate whether the observed delay in migration of *tau −/−map1b −/−* neurons is dependent on the suppression of neurite elongation. No significant difference in mean migration index was observed between *tau +/+map1b +/+* and *tau −/−map1b −/−* aggregates (Table VIII; $P > 0.2$ by Student's *t* test), suggesting that the inhibition of neuronal migration of *tau −/− map1b −/−* neurons was due to the suppression of neurite elongation.

Table VIII. Neurite Length and Migration Indices of Cerebellar Granule Cells

	Neurite length	Migration index
	μm	
tau +/+map1b +/+	652 ± 14*	0.42 ± 0.03
tau −/−map1b −/−	531 ± 12	0.37 ± 0.03

Neurite length is defined as the average length of the longest neurite on each aggregate. The migration index is defined as the ratio of the number of neurons that migrated beyond one-third of the neurite length to the total number of migrating neurons. The means ± SEM are shown. Three animals of each genotype were used, and 35 *tau +/+map1b +/+* and 33 *tau −/−map1b −/−* clusters were examined.
*Differs from *tau −/−map1b −/−* at $P < 0.001$ using Student's *t* test.

Discussion

Tau and MAP1B Act Cooperatively in Neuronal Morphogenesis

A great deal of interest has been focused on the cytoskeletal basis of neuronal development. Although tau and MAP1B have been implicated in the process, the functions of tau and MAP1B in vivo remain controversial.

In the analysis of mice with a genetic background of predominantly C57Bl/6J (>93%), *tau +/+map1b −/−* mice have a partial postnatal lethality. A hypoplastic commissural axon tract and disorganized neuronal layering were observed in their brains, indicating the importance of MAP1B in axonal development and neuronal layer formation. These phenotypes are markedly more severe in the *tau −/−map1b −/−* double mutant, demonstrating the syn-

ergistic effects of *tau* and *map1b* mutations on neuronal morphogenesis.

Role of tau and MAP1B in Axonal Elongation

In *tau*−/−*map1b*−/− mice, major commissural fibers such as the corpus callosum and anterior commissure were severely affected. Noncommissural long tracts in the cerebellum and the spinal cord were also hypoplastic. Electron microscopy revealed a decrease in the cross-sectional area of axons, which means that reduction in size of the axon tracts was mainly due to defective development of neuronal axons, and not of other cellular components such as glial cells. This assumption is supported by observations in the cultured hippocampal neurons, which indicate that defects in axon tract formation are cell-autonomous and can be satisfactory explained by inhibition of nerve growth.

In *tau*+/+*map1b*−/− and *tau*−/−*map1b*−/− cultures, minor process elongations were also affected. As no significant difference in the minor process length was observed between *tau*+/+*map1b*−/− and *tau*−/−*map1b*−/− cultures, the mutation of *map1b* gene is considered to be mainly responsible for this phenotype.

Tau and MAP1B Are Involved in the Organization of MTs in Growth Cones

Growth cone translocation is a key event in axonal elongation. The sequence of cytoskeleton-dependent advance of the growth cone can be subdivided into the following four stages (Mitchison and Kirschner, 1988; Tanaka and Sabry, 1995). Stage of exploration (stage 1): during this stage, the filopodia and lamella in the growth cones are highly dynamic, and their shapes are mainly determined by the organization of actin microfilaments within them. MTs are localized in the central domain of the growth cone. Stage of MT invasion (stage 2): MTs invade into the periphery of the growth cone. Stage of stabilization (stage 3): MTs are organized to form a bundle in the growth cone. Stage of axon formation (stage 4): the plasma membrane of the growth cone collapses around the MT bundle to generate a new axon tube.

We found abnormalities in the shape and cytoskeletal organization of growth cones in *tau*−/−*map1b*−/− mice. Their MT-rich central domain was often extended, and the MTs were splayed into single MTs with little tendency toward bundle formation. These findings strongly indicate that stages 3 and 4 are selectively disturbed in the affected growth cones. In normally developing neurons, tau and MAP1B are colocalized with MTs in the growth cones (Black et al., 1994, 1996), and are components of the filamentous structures that form crossbridges between the MTs (Hirokawa et al., 1988; Sato-Yoshitake et al., 1989). When transfected to non-neuronal cells, they induce reorganization of the MT network into bundle formation (Kanai et al., 1989; Chen et al., 1992) and reduce MT spacing (Tögel et al., 1998). Taken collectively, it is considered that the activity of these MAPs zips MTs at the neck of the advancing growth cones, and converts the dynamic MTs into highly organized parallel arrays of axonal MTs (Fig. 9). Our data also suggest that the coalescence of the plasma membrane cortex at stage 4 requires prior bundle formation of the MTs.

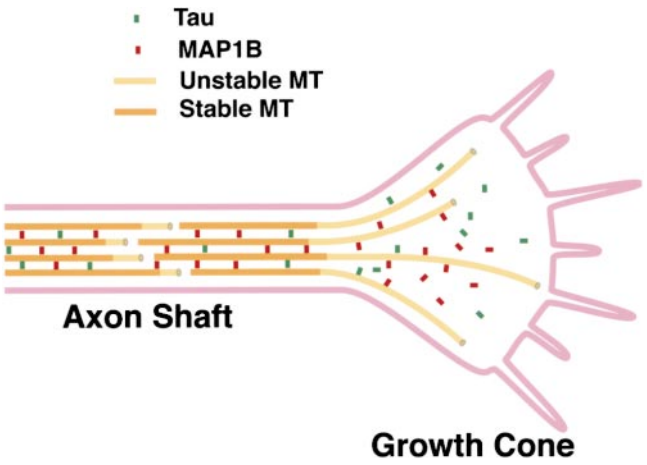

Figure 9. Schematic diagram of growth cones showing the role of tau and MAP1B in organizing MTs in growth cones. Tau and MAP1B are considered to zip MTs in the advancing growth cones, and convert the dynamic MTs into highly organized parallel arrays of axonal MTs.

Role of MAPs in Neuronal Migration

Another noteworthy finding of our study was the disruption of neuronal layer formation in vivo and a delayed neuronal migration in vitro. This suggests that tau and MAP1B are involved not only in axonal extension, but also in the motile behavior of migrating neurons as MT organizers.

In neuronal migration, a nuclear displacement within the leading process follows process formation. A coordinated organization of actin microfilaments and MTs is required in this process (Rivas and Hatten, 1995; Rakic et al., 1996). Recently, LIS1 and Doublecortin (DCX) were shown to relate with MT organization in migrating neurons. DCX, a product of *doublecortin* gene that is responsible for X-linked lissencephaly, binds to and stabilizes MTs (Francis et al., 1999; Gleeson, et al., 1999), and LIS1, which is defective in cases with Miller-Dieker lissencephaly, reduces catastrophic events of MTs (Sapir et al., 1997). A *Lis1* homologue in *Aspergillus nidulans*, *nudF*, affects nuclear migration by acting on the dynein motor system (Morris et al., 1998).

We observed a delay in neuronal migration with a concomitant suppression in leading process elongation in *tau*−/−*map1b*−/− reaggregate clusters, which suggests that tau and MAP1B act primarily on leading process elongation, not in nuclear displacement during neuronal migration.

Future Directions

Recent studies indicate that tau or MAP1B interacts with non-MT cellular components. Tau interacts with a neural plasma membrane through its projection domain (Brandt et al., 1995). MAP1B is associated with actin filaments (Tögel et al., 1998) and a membrane receptor GABA(C) (Hanley et al., 1999). We found an altered F-actin localization, as indicated by the absence of phalloidin staining in the central MT-rich domain, in mutant growth cones. We

cannot conclude for certain whether this directly reflects the loss of tau and MAP1B functions, or is a secondary effect resulting from altered MT dynamics caused by the lack of MAPs. Further experiments will be required to characterize changes in actin filaments or plasma membrane dynamics in MAP-deficient neurons.

We thank S. Terada-Inomata, S. Nonaka, T. Nakata, N. Honma, H. Sato, N. Ono-uchi, M. Sugaya-Otsuka, and H. Fukuda (University of Tokyo) for their help.

This work was supported by a grant for Center of Excellence (COE) to N. Hirokawa.

Submitted: 13 March 2000
Revised: 29 June 2000
Accepted: 18 July 2000

References

Bix, G.J., and G.D. Clerk. 1998. Platelet-activating factor receptor stimulation disrupts neuronal migration in vivo. *J. Neurosci.* 18:307–318.

Black, M.M., T. Slaughter, and I. Fischer. 1994. Microtubule-associated protein 1b (MAP1b) is concentrated in the distal region of growing axons. *J. Neurosci.* 14:857–870.

Black, M.M., T. Slaughter, S. Moshiach, M. Obrocka, and I. Fischer. 1996. Tau is enriched on dynamic microtubules in the distal region of growing axons. *J. Neurosci.* 16:3601–3619.

Bloom, G.S., F.C. Luca, and R.B. Vallee. 1985. Microtubule-associated protein 1B: identification of a major component of the neuronal cytoskeleton. *Proc. Natl. Acad. Sci. USA*. 82:5404–5408.

Bodian, P.A. 1936. A new method for staining nerve fibers and nerve endings in mounted paraffin sections. *Anat. Rec.* 65:89–96.

Brandt, R., J. Leger, and G. Lee. 1995. Interaction of tau with the plasma membrane mediated by tau's amino-terminal projection domain. *J. Cell Biol.* 131: 1327–1340.

Brugg, B., D. Reddy, and A. Matus. 1993. Attenuation of microtubule-associated protein 1B expression by antisense oligonucleotides inhibits initiation of neurite outgrowth. *Neuroscience.* 52:489–496.

Caceres, A., and K.S. Kosik. 1990. Inhibition of neurite polarity by tau antisense oligonucleotides in primary cerebellar neurons. *Nature.* 343:461–463.

Caceres, A., S. Potrevic, and K.S. Kosik. 1991. The effect of tau antisense oligonucleotides on neurite formation of cultured cerebellar macroneurons. *J. Neurosci.* 11:1515–1523.

Chen, J., Y. Kanai, N.J. Cowan, and N. Hirokawa. 1992. Projection domains of MAP2 and tau determine spacings between microtubules in dendrites and axons. *Nature.* 360:674–677.

Cleveland, D.W., S.Y. Hwo, and M.W. Kirschner. 1977. Purification of tau, a microtubule-associated protein that induces assembly of microtubules from purified tubulin. *J. Mol. Biol.* 116:207–225.

DiTella, M.C., F. Feiguin, N. Carri, K.S. Kosik, and A. Caceres. 1996. MAP-1B/TAU functional redundancy during laminin-enhanced axonal growth. *J. Cell Sci.* 109:467–477.

Dotti, C.G., C.A. Sullivan, and G.A. Banker. 1988. The establishment of polarity by hippocampal neurons in culture. *J. Neurosci.* 8:1454–1468.

Edelmann, W., M. Zervas, P. Costello, L. Roback, I. Fischer, A. Hammarback, N. Cowan, P. Davis, B. Wainer, and R. Kucherlapati. 1996. Neuronal abnormalities in microtubule-associated protein 1B mutant mice. *Proc. Natl. Acad. Sci. USA*. 93:1270–1275.

Francis, F., A. Koulakoff, D. Boucher, P. Chafey, B. Schaar, M.-C. Vinet, G. Friocourt, N. McDonnell, O. Reiner, A. Kahn, et al. 1999. Doublecortin is a developmentally regulated, microtubule-associated protein expressed in migrating and differentiating neurons. *Neuron.* 23:247–256.

Gleeson, J.G., P.T. Lin, L.A. Flanagan, and C.A. Walsh. 1999. Doublecortin is a microtubule-associated protein and is expressed widely by migrating neurons. *Neuron.* 23:257–271.

Hanley, J.G., P. Koulen, F. Bedford, P.R. Gordon-Weeks, and S.J. Moss. 1999. The protein MAP1B links GABA(C) receptors to the cytoskeleton at retinal synapses. *Nature.* 397:66–69.

Harada, A., K. Oguchi, S. Okabe, J. Kuno, S. Terada, T. Ohshima, R. Sato-Yoshitake, Y. Takei, T. Noda, and N. Hirokawa. 1994. Altered microtubule organization in small-calibre axons of mice lacking tau protein. *Nature.* 369: 488–491.

Hirokawa, N. 1982. The crosslinker system between neurofilaments, microtubules and membranous organelles in frog axons revealed by quick freeze, freeze fracture, deep etching method. *J. Cell Biol.* 94:425–443.

Hirokawa, N. 1994. Microtubule organization and dynamics dependent on microtubule-associated proteins. *Curr. Opin. Cell Biol.* 6:74–81.

Hirokawa, N., G.S. Bloom, and R.B. Vallee. 1985. Cytoskeletal architecture and immunocytochemical localization of microtubule-associated proteins in regions of axons associated with rapid axonal transport: the IDPN-intoxicated axon as a model system. *J. Cell Biol.* 101:1858–1870.

Hirokawa, N., Y. Shiomura, and S. Okabe. 1988. Tau proteins: the molecular structure and mode of binding on microtubules. *J. Cell Biol.* 107:1449–1461.

Hummel, T., K. Krukkert, J. Roos, G. Davis, and C. Klämbt. 2000. *Drosophila* Futsch/22C10 is a MAP1B-like protein required for dendritic and axonal development. *Neuron.* 26:357–370.

Ikegami, S., A. Harada, and N. Hirokawa. 2000. Muscle weakness, hyperactivity, and impairment in fear conditioning in tau-deficient mice. *Neurosci. Lett.* 279:129–132.

Kanai, Y., R. Takemura, T. Ohshima, H. Mori, Y. Ihara, M. Yanagisawa, T. Masaki, and N. Hirokawa. 1989. Expression of multiple tau isoforms and microtubule bundle formation in fibroblasts transfected with a single tau cDNA. *J. Cell Biol.* 109:1173–1184.

Kobayashi, S., K. Isa, K. Hayashi, H.K. Inoue, K. Uyemura, and T. Shirao. 1995. K252a, a potent inhibitor of protein kinases, inhibits the migration of cerebellar granule cells in vitro. *Dev. Brain Res.* 90:122–128.

Liu, C.A., G. Lee, and D.G. Jay. 1999. Tau is required for neurite outgrowth and growth cone motility of chick sensory neurons. *Cell Motil. Cytoskel.* 43: 232–242.

Mitchison, T., and M. Kirschner. 1988. Cytoskeletal dynamics and nerve growth. *Neuron.* 1:761–772.

Morris, N.R., V.P. Efimov, and X. Xiang. 1998. Nuclear migration, nucleokinesis and lissenchephaly. *Trends Cell Biol.* 8:467–470.

Noble, M., S.A. Lewis, and N.J. Cowan. 1989. The microtubule-binding domain of microtubule-associated protein MAP1B contains a repeated sequence motif unrelated to that of MAP2 and tau. *J. Cell Biol.* 109:3367–3376.

Rakic, P., E. Knyihar-Csillik, and B. Csillik. 1996. Polarity of microtubule assemblies during neuronal cell migration. *Proc. Natl. Acad. Sci. USA*. 93: 9218–9222.

Rivas, R.J., and M.E. Hatten. 1995. Motility and cytoskeletal organization of migrating cerebellar granule neurons. *J. Neurosci.* 15:981–989.

Sapir, T., M. Elbaum, and O. Reiner. 1997. Reduction of microtubule catastrophe events by LIS1, a platelet activating factor acetylhydrolase subunit. *EMBO (Eur. Mol. Biol. Organ.) J.* 16:6977–6984.

Sato-Yoshitake, R., Y. Shiomura, H. Miyasaka, and N. Hirokawa. 1989. Microtubule-associated protein 1B: molecular structure, localization, and phosphorylation-dependent expression in developing neurons. *Neuron.* 3:229–238.

Takei, Y., S. Kondo, A. Harada, S. Inomata, T. Noda, and N. Hirokawa. 1997. Delayed development of nervous system in mice homozygous for disrupted microtubule-associated protein 1B (MAP1B) gene. *J. Cell Biol.* 137:1615–1626.

Tanaka, E., and J. Sabry. 1995. Making connection: cytoskeletal rearrangements during growth cone guidance. *Cell.* 83:171–176.

Tanaka, Y., K. Kawahata, T. Nakata, and N. Hirokawa. 1992. Chronological expression of microtubule-associated proteins (MAPs) in EC cell P19 after neuronal induction by retinoic acid. *Brain Res.* 596:269–278.

Tint, I., T. Slaughter, I. Fischer, and M.M. Black. 1998. Acute inactivation of tau has no effect on dynamics of microtubules in growing axons of cultured sympathetic neurons. *J. Neurosci.* 18:8660–8673.

Tögel, M., W. Gerhard, and F. Propst. 1998. Novel features of the light chain of microtubule-associated protein MAP1B: microtubule stabilization, self-interaction, actin filament binding, and regulation by the heavy chain. *J. Cell Biol.* 143:695–707.

Trommsdorff, M., M. Gotthardt, T. Hiesberger, J. Shelton, W. Stockinger, J. Nimph, R.E. Hammer, J.A. Richardson, and J. Herz. 1999. Reeler/Disabled-like disruption of neuronal migration in knockout mice lacking the VLDL receptor and ApoE receptor 2. *Cell.* 97:689–701.

Ulloa, L., J. Diaz-Nido, and J. Avila. 1993. Depletion of casein kinase II by antisense oligonucleotide prevents neuritogenesis in neuroblastoma cells. *EMBO (Eur. Mol. Biol. Organ.) J.* 12:1633–1640.

Wahlsten, D. 1989. Genetic and developmental defects of the mouse corpus callosum. *Experientia.* 45:828–838.